Electron impact ionization and dissociation of CO_2^+ to C^+ and O^+

2001 J. Phys. B: At. Mol. Opt. Phys. 34 1757

(http://iopscience.iop.org/0953-4075/34/9/312)

INSTITUTE OF PHYSICS PUBLISHING JOURNAL OF PHYSICS B: ATOMIC, MOLECULAR AND OPTICAL PHYSICS

J. Phys. B: At. Mol. Opt. Phys. **34** (2001) 1757–1767 www.iop.org/Journals/jb PII: S0953-4075(01)19100-5

Electron impact ionization and dissociation of CO_2^+ to C^+ and O^+

E M Bahati[1], J J Jureta[1,2], D S Belic[1,3], S Rachafi[1,4] and P Defrance[1]

[1] Université Catholique de Louvain, Département de Physique, Chemin du Cyclotron, 2, B-1348 Louvain-la Neuve, Belgium
[2] Institute of Physics, PO Box 68, 11081 Beograd, Yugoslavia
[3] Faculty of Physics, PO Box 550, 11000 Beograd, Yugoslavia
[4] Faculté des Sciences, Unité IMC, Université Chouaïb Doukkali, BP 20 El Jadida, Morocco

Received 15 November 2000, in final form 26 February 2001

Abstract

Absolute cross sections for electron impact ionization and dissociation of CO_2^+ to form C^+ and O^+ fragments are measured in the energy range from threshold to 2500 eV. The animated crossed-beams method has been employed. The ionization cross section shows a maximum of 4.79×10^{-17} cm^2 at 130 eV and the corresponding threshold is found in good agreement with previous measurements. Both dissociation cross sections are shown to exhibit wide plateaux which are of the same order of magnitude. In addition, these cross sections almost coincide above 100 eV. The threshold energy and kinetic energy released are determined for both the production of C^+ and O^+. They are found in good agreement with the previously published data obtained in electron impact ionization experiments of neutral CO_2.

1. Introduction

Electron collisions with molecular ions may be present in many laboratory or natural plasmas. Due to their complex structure, these systems are difficult to handle, both experimentally and theoretically. Experimentally, it is hard to produce a beam of ions in the ground state or in a specific excited state and, in dissociation processes, particular difficulties are associated with the collection of energetic fragments. In the cases where product ions have identical charge-to-mass ratios (O^+, O_2^{2+}) and average velocities, they cannot be separated by classical analysing devices. As a consequence, the number of reported investigations in this field is still limited.

Electron impact ionization of molecular ions has been studied so far only for CO_2^+ (Müller *et al* 1980) and for CO^+ (Belic *et al* 1997), to our knowledge. Concerning dissociative processes (excitation and ionization) of molecular ions, experiments (Dunn and Van Zyl 1967) and calculations (Peek 1967) were first performed for H_2^+. Since then, experiments have been performed for diatomic ions, homonuclear (N_2^+ and O_2^+: Van Zyl and Dunn (1967), Siari *et al* (1999)) or heteronuclear (Mitchell and Hus 1985, Djuric *et al* 1997, Belic *et al* 1997), and for polyatomic ions (Schulz *et al* 1986, Van der Donk *et al* 1991). Related information is given by Tian and Vidal (1998), Velotta *et al* (1994) and Locht and Davister (1995) who have

0953-4075/01/091757+11$30.00

investigated the kinetic energy and angular distributions of the fragments from electron impact dissociation of neutral CO_2. Quite recently, the merging beam method has been implanted on ion storage rings for the study of dissociative processes (Forck *et al* 1993, Andersen *et al* 1996, Peterson *et al* 1998). It is worth mentioning that no theoretical result is presently available either for ionization, or for dissociation.

In collisions with energetic electrons, the CO_2^+ molecular ion may undergo various inelastic processes of ionization (1), dissociative ionization ($2a$)–($2f'$) (if dissociation follows ionization) and dissociative excitation ($3a$)–($3d$):

$$e^- + CO_2^+ \rightarrow CO_2^{2+} + 2e^- \tag{1}$$

$$\hookrightarrow C^+ + O_2^+ \tag{2a}$$
$$\hookrightarrow O^+ + CO^+ \tag{2b}$$
$$\hookrightarrow C^{2+} + O_2 \tag{2c}$$
$$\hookrightarrow O^{2+} + CO \tag{2d}$$
$$\hookrightarrow C + O_2^{2+} \tag{2e}$$
$$\hookrightarrow O^+ + O^+ \tag{2e'}$$
$$\hookrightarrow O + CO^{2+} \tag{2f}$$
$$\hookrightarrow C^+ + O^+ \tag{2f'}$$

$$\rightarrow C^+ + O_2 + e^- \tag{3a}$$
$$\rightarrow O^+ + CO + e^- \tag{3b}$$
$$\rightarrow O_2^+ + C + e^- \tag{3c}$$
$$\rightarrow CO^+ + O + e^-. \tag{3d}$$

The doubly charged CO_2^{2+} ion spontaneously decays following the various dissociative ionization channels. In addition, the other doubly charged products O_2^{2+} and CO^{2+} may further dissociate after some time.

In this paper, we report on cross section measurements for the formation of CO_2^{2+} (1), C^+ ($2a$), ($2f'$) and ($3a$) and O^+ ($2b$), ($2e'$), ($2f'$) and ($3b$) from threshold to about 2500 eV.

In section 2, the experimental method and the apparatus are described. Section 3 is devoted to the analysis of dissociation products. Results are presented and discussed in section 4.

2. Experimental method and apparatus

Measurements are performed by use of the animated crossed-beams apparatus described elsewhere (Defrance *et al* 1981, Zambra *et al* 1994). The ion beam transport line was recently modified. Figure 1 shows the present experimental set-up. CO_2^+ ions are extracted from a Penning ion source (PIG), and accelerated to 4 keV. The ion beam is selected by means of a 90° magnetic analyser, additionally focused and purified by a 45° electrostatic spherical deflector, and directed into the collision region. The ribbon-shaped electron beam is produced by a Pierce-type cathode–anode configuration. It is focused in the collision region where it crosses the ion beam, at right angle. A pair of parallel plates acts simultaneously as a lens and as the beam deflector needed for the application of the animated beam method. During the measurements, the electron beam is swept across the ion beam in a linear see-saw motion, at a constant velocity. This velocity is measured by means of two thin wires located on either side of the ion beam symmetrically, perpendicular to the electron beam trajectory.

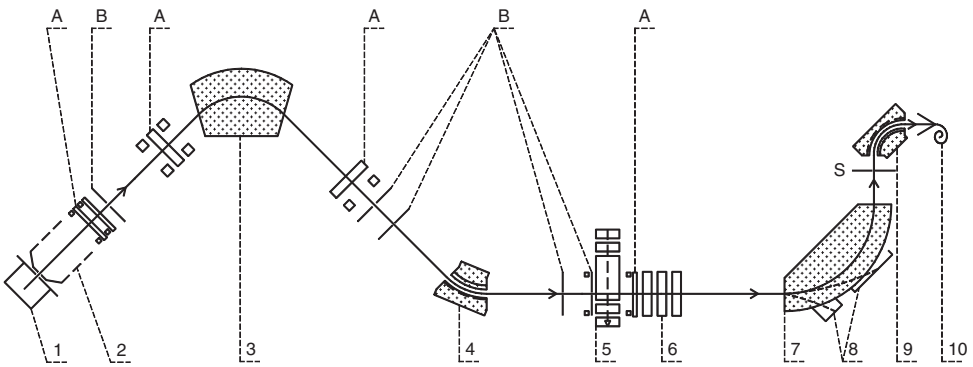

Figure 1. Experimental set-up. (1) Ion source; (2) electrostatic lens; (3) magnetic analyser; (4) spherical deflector; (5) electron gun; (6) vertical lens; (7) analysing magnet; (8) Faraday cup; (9) spherical deflector; (10) channeltron detector; (A) electrostatic deflectors; (B) diaphragms; (S) slit.

After the collision, product ions are focused by a vertical einzel lens and separated from the primary ion beam by means of a 90° magnetic analyser. A positive voltage (300 V) is applied to the electrodes surrounding the interaction region so that the energy of positive ions formed inside this region is increased. Ions formed outside this region do not undergo this kinetic displacement and are rejected by the magnetic analyser. The primary ion beam is detected by a wide Faraday cup, located inside the magnetic field. Product ions are further deflected by a 90° electrostatic spherical deflector and directed onto a channeltron detector.

From the measured quantities the cross section is determined by the following expression:

$$\sigma = \frac{v_e v_i}{(v_e + v_i)^{1/2}} \frac{e^2 q}{I_e I_i} \frac{uK}{D} \tag{4}$$

where u is the electron beam scanning velocity, K is the total number of events produced during one passage of electrons across the ion beam, D is the detector efficiency, v_e and v_i, I_e and I_i, e and q represent the velocities, currents and charges of electrons and ions, respectively. All the slits and apertures between the collision region and the ion detector are dimensioned so as to provide the total ion transmission in ionization experiments. However, this is not the case for dissociation fragments. This will be discussed in more detail later. In ionization experiments, the signal-to-background ratio is very high (≈200) at high electron energy. In the case of dissociation, the background count rate is much higher and the signal-to-background ratio is of the order of 0.01 only. Measurements required a longer time to reach acceptable statistical uncertainties.

3. Detection of dissociation fragments

When dissociation takes place, internal potential energy may be transformed into kinetic energy of fragments. In the laboratory frame, these fragments exhibit angular and energy distributions which are larger than the primary beam distributions. The angular dispersion is cancelled by the analysing magnet focusing properties and by a vertical lens located at the exit of the collision region. However, at the exit of the analysing magnet (7, figure 1), the spatial distribution of energetic fragments in the dispersion (horizontal) plane is too large to ensure their total collection. The vertical slit (S), placed between the magnet and the electrostatic spherical deflector (9), determines the actual fraction of detected fragments. This

slit is wide enough to provide total transmission of direct ionization products, either atomic or molecular. This is confirmed by a careful scan of the signal with the analysing magnetic field. The signals exhibit a wide plateau, which is the usual test for total collection of ions. This type of test is systematically performed for all the focusing or deflecting ion transport elements.

The energy distribution or the actual size of the beam is deduced from the derivative of the observed spectrum. For the ionization products (or for the primary ion beam) this size is usually smaller than the width of the slit, providing total collection. For the dissociation fragments, however, the spectrum resulting from the magnetic field scan is much wider and does not exhibit a plateau, indicating that the size of the beam is larger than the slit. Subsequently, only a fraction of charged fragments is collected at any beam position, i.e. at any value of the analysing magnetic field. This needs to be accounted for in order to determine the corresponding absolute cross section. The ratio of collected and actual number of particles is referred to as the transmission efficiency. It needs to be determined for each dissociative process. The corresponding procedure has been described previously (Belic and Defrance 1998, Siari *et al* 1999) and only a short outline is given here.

Let us consider briefly the dynamics of dissociation fragments. The energy of a fragment ion (A^+) in the laboratory frame is given by

$$E_A = \frac{m_A}{M}(E_M - q_M V_b) + \frac{\mu}{m_A}\Delta E_{CM} \pm 2\cos\theta\sqrt{\frac{\mu}{M}(E_M - q_M V_b)\Delta E_{CM}} + q_A V_b \qquad (5)$$

where E_M, M, q_M are the energy, mass and charge of the primary molecular ion, respectively. m_A and q_A are the mass and the charge of the fragment and μ is the reduced mass. ΔE_{CM} is the internal energy converted into kinetic energy released (KER) to fragments and θ is the emission angle of fragments with respect to the primary ion beam velocity. V_b is the collision region bias potential. From (5), it can be seen that the energy difference between fragments emitted forward ($\theta = 0$) and backward ($\theta = \pi$) may be large (several tens of eV) even if ΔE_{CM} is small (a few eV). That difference represents the width of the product energy distribution which is unknown but can be deduced from the magnetic field scan. A transformation of this distribution, according to the finite width of the slit, leads to the transmission efficiency. The procedure is correct under the assumption that the scan occurs only within a few per cent of the actual magnetic field strength, which is true in the present case.

The transmission efficiency was found to be 57% and 34% for C^+ and for O^+, respectively. Furthermore, ΔE_{CM} may be estimated from the width of the energy profile. At 120 eV incident electron energy, estimations are 3.0 and 8.7 eV for C^+ and O^+ respectively. For O^+ production at 30 eV, ΔE_{CM} is found to be 4.9 eV only.

The total absolute uncertainties for these measurements are obtained as the quadrature sum of uncertainties on all measured quantities: counting statistics ($\leqslant \pm 1\%$), sweeping velocity ($\pm 2\%$), electron current ($\pm 1\%$), ion current ($\pm 1\%$) and detector efficiency ($\pm 1.7\%$). For ionization, the total uncertainty is $\pm 5\%$. For dissociation, the additional uncertainty due to the transmission efficiency estimation is of the order of $\pm 6\%$ for C^+ and $\pm 10\%$ for O^+, leading to total uncertainties of $\pm 11\%$ and $\pm 15\%$, respectively. The difference in these uncertainties is due to the signal-to-noise ratio which is of the order of 50% for C^+ and a few per cent only for O^+. The electron energy in our experiment was calibrated against the well known spectroscopic value for singly charged argon ion ionization, in a separate experiment. The actual electron energy is corrected for contact potentials and for ion velocity. The error on the true collision energy is ± 0.5 eV.

Table 1. Absolute cross sections for CO_2^{2+}, C^+ and O^+ production

E_e (eV)	$\sigma_{CO_2^{2+}}$ (10^{-17} cm^2)	$\Delta\sigma_{CO_2^{2+}}$ (10^{-17} cm^2)	σ_{C^+} (10^{-17} cm^2)	$\Delta\sigma_{C^+}$ (10^{-17} cm^2)	σ_{O^+} (10^{-17} cm^2)	$\Delta\sigma_{O^+}$ (10^{-17} cm^2)
3.4	—	—	—	—	−0.11	0.1
3.9	—	—	—	—	0.01	0.1
4.4	—	—	—	—	0.05	0.2
4.9	—	—	—	—	−0.02	0.2
5.4	—	—	—	—	0.2	0.2
5.9	—	—	—	—	0.6	0.1
6.4	—	—	—	—	0.9	0.1
6.9	—	—	—	—	1.3	0.1
7.9	—	—	—	—	1.7	0.2
8.9	—	—	−0.01	0.01	2.1	0.3
9.9	—	—	0.1	0.03	2.4	0.2
10.9	—	—	0.03	0.02	2.5	0.2
11.9	—	—	0.1	0.02	2.9	0.2
12.9	—	—	0.1	0.03	3.2	0.2
13.9	—	—	0.2	0.03	3.4	0.3
14.9	—	—	0.4	0.04	3.4	0.1
15.9	—	—	0.6	0.03	—	—
16.9	—	—	1.0	0.04	3.5	0.1
17.9	—	—	1.5	0.1	—	—
18.9	—	—	1.8	0.1	3.6	0.1
20.9	—	—	2.5	0.1	3.7	0.2
22.9	0.00	0.00	2.8	0.04	3.8	0.2
23.9	0.00	0.00	—	—	—	—
24.9	0.07	0.01	3.1	0.1	3.9	0.1
25.9	0.18	0.01	—	—	—	—
26.9	0.32	0.01	3.2	0.1	—	—
27.9	0.43	0.01	—	—	—	—
28.9	0.56	0.01	3.4	0.1	3.9	0.2
30.9	0.83	0.01	3.4	0.1	—	—
32.9	1.09	0.01	—	—	—	—
33.9	—	—	—	—	3.8	0.2
34.9	1.49	0.01	3.4	0.1	—	—
36.9	1.60	0.01	—	—	—	—
38.9	1.83	0.01	3.4	0.1	3.8	0.1
40.9	2.07	0.01	—	—	—	—
43.9	—	—	3.4	0.1	3.8	0.1
44.9	2.49	0.01	—	—	—	—
48.9	2.92	0.01	3.4	0.1	3.7	0.1
53.9	3.32	0.01	3.4	0.1	3.7	0.1
58.9	3.56	0.01	3.4	0.03	3.7	0.1
63.9	3.81	0.01	—	—	—	—
68.9	4.07	0.01	3.5	0.03	3.7	0.04
73.9	4.26	0.01	—	—	—	—
78.9	4.38	0.01	3.5	0.03	3.7	0.1
88.9	4.58	0.01	3.5	0.03	3.5	0.1
98.9	4.67	0.01	3.4	0.02	3.5	0.1
108.9	4.76	0.01	—	—	3.4	0.04
118.9	4.78	0.01	3.3	0.02	3.4	0.1
128.9	4.79	0.01	—	—	—	—
138.9	4.75	0.01	3.2	0.02	3.1	0.1
148.9	4.74	0.01	—	—	—	—

Table 1. (Continued.)

E_e (eV)	$\sigma_{CO_2^{2+}}$ (10^{-17} cm^2)	$\Delta\sigma_{CO_2^{2+}}$ (10^{-17} cm^2)	σ_{C^+} (10^{-17} cm^2)	$\Delta\sigma_{C^+}$ (10^{-17} cm^2)	σ_{O^+} (10^{-17} cm^2)	$\Delta\sigma_{O^+}$ (10^{-17} cm^2)
158.9	4.70	0.01	3.04	0.01	3	0.1
178.9	4.61	0.01	2.9	0.01	2.9	0.1
198.9	4.47	0.01	2.8	0.01	2.8	0.04
228.9	4.26	0.01	2.5	0.01	2.5	0.04
258.9	4.08	0.01	2.3	0.01	2.3	0.04
298.9	3.38	0.01	2.2	0.01	2.1	0.03
348.9	3.63	0.01	2.0	0.01	1.9	0.03
398.9	3.38	0.01	1.8	0.01	1.7	0.04
448.9	3.22	0.01	1.7	0.01	—	—
498.9	3.06	0.01	1.6	0.01	1.6	0.03
598.9	2.85	0.01	1.4	0.01	1.4	0.03
698.9	2.63	0.01	1.3	0.01	1.2	0.03
798.9	2.45	0.01	1.2	0.01	1.2	0.04
898.9	2.27	0.01	1.1	0.01	1.1	0.03
998.9	2.13	0.01	1.02	0.01	1	0.02
1298.9	1.82	0.01	0.9	0.01	0.8	0.02
1598.9	1.58	0.01	0.7	0.01	0.7	0.02
1998.9	1.37	0.01	0.6	0.01	0.6	0.02
2498.9	1.18	0.01	0.5	0.01	0.5	0.02

4. Results and discussion

Absolute cross sections for electron impact single ionization of CO_2^+ and for production of C^+ and O^+ fragments are measured in the energy range from threshold to 2500 eV. Results are listed in table 1 together with electron energies and corresponding statistical uncertainties. Identical product fragments are detected regardless of their origin. As a consequence, C^+ and O^+ ions produced in various reaction channels (2) and (3) cannot be resolved in the present experiment.

4.1. Ionization

Absolute cross sections for electron impact ionization of CO_2^+ are presented in figure 2. The cross section maximum is 4.79×10^{-17} cm^2 at 130 eV. In this case, the statistical error bars are very small and cannot be distinguished on the figure.

Müller *et al* (1980) measured the cross sections for this process and their data are also shown in the figure. Error bars corresponding to the total absolute uncertainty (95% confidence level), are presented for these data and for three electron energies (present results). The accuracy of both sets of data is similar and the two sets of data agree reasonably in the whole energy range, but our cross sections are systematically higher, by some 15% near the maximum. This discrepancy could result from the sum of errors affecting the experimental parameters. However, it is more likely to be due to (i) small differences between the respective distributions of metastable excited states for the target ions in the collision region or (ii) to the finite lifetime against dissociation of CO_2^{2+} product ions.

The absence of any signal below the ionization threshold in both experiments indicates that electronically excited states do not contribute to the recorded signal. As for vibrationally excited states, their presence is not expected to significantly influence the cross section and, in addition, they are difficult to observe in the threshold region due to the very small energy displacement involved.

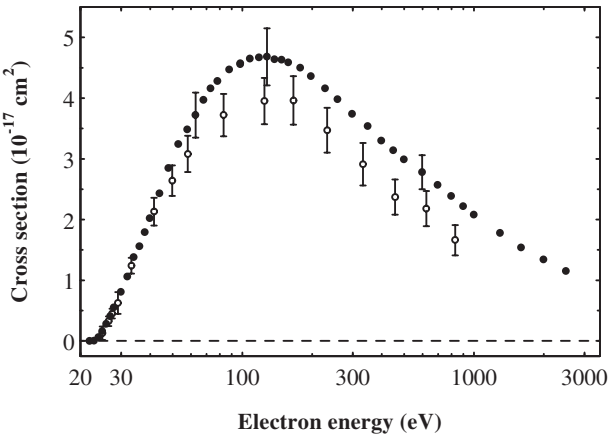

Figure 2. Absolute cross sections for single ionization of CO_2^+: (●) present data; (○), Müller *et al* (1980).

Due to their finite lifetime, part of the CO_2^{2+} ions evolve through dissociative ionization (DI) reactions $(2a)$–$(2f)$ and cannot be detected. This effect should reduce the measured ionization cross section. The lifetime was subject to several investigations. Newton and Sciamanna (1964) reported a mean lifetime of (3.3 ± 0.3) μs, Tsai and Eland (1980) of 21.6 μs and Field and Eland (1993) of 0.9 μs. It seems likely that several metastable states are involved with different characteristics. The transit times of CO_2^{2+} ions to the detector differ in both experiments. In the present experiment, the ion energy is varied from 4.3 to 1.3 keV, corresponding to dication transit times of 11.2 and 21.1 μs, respectively. In the experiment of Müller *et al* (1980) the transit times were 5.4 and 3.8 μs for 5 and 10 keV ions, respectively. No significant change in the cross section magnitude was observed when varying the ion energy in each experiment. In addition, the cross sections of Müller *et al* (1980) should be higher rather than lower than the present ones due to shorter transit time. Finally, none of these tests allow the effect of finite lifetime to be observed and the discrepancy between the data remains unexplained.

The experimental ionization threshold energy for CO_2^+ is found to be (23.9 ± 0.5) eV, a value which is in good agreement with existing data. Müller *et al* (1980) obtained a value of (23.4 ± 0.6) eV. The threshold energy for CO_2 ionization was determined by spectroscopic methods (Dibeler 1967, 1968, McCulloh 1973) and established at 13.8 eV. In mass spectrometry experiments, the double-ionization threshold was found to be (36.4 ± 1) eV by Bussières and Marmet (1977) and (37.2 ± 0.5) eV by Märk and Hille (1978), relative to the ground state of the neutral CO_2 molecule. In a threshold photo-electron coincidence spectroscopy, Hall *et al* (1992) obtained (37.3 ± 0.1) eV.

There are no theoretical cross section predictions for this process, to our knowledge, which can be compared with the present data.

4.2. C^+ production

C^+ ions are formed from DI or dissociative excitation (DE) reactions $(2a)$, $(2f')$ or $(3a)$. In these cases a number of particular molecular states may be involved, which results in a significantly enlarged energy distribution of fragments in the laboratory frame. This can be seen from a scan of the apparent cross section with the analysing magnetic field. Such a scan, obtained at 120 eV incident electron energy, is shown in figure 3(a). It extends from 570

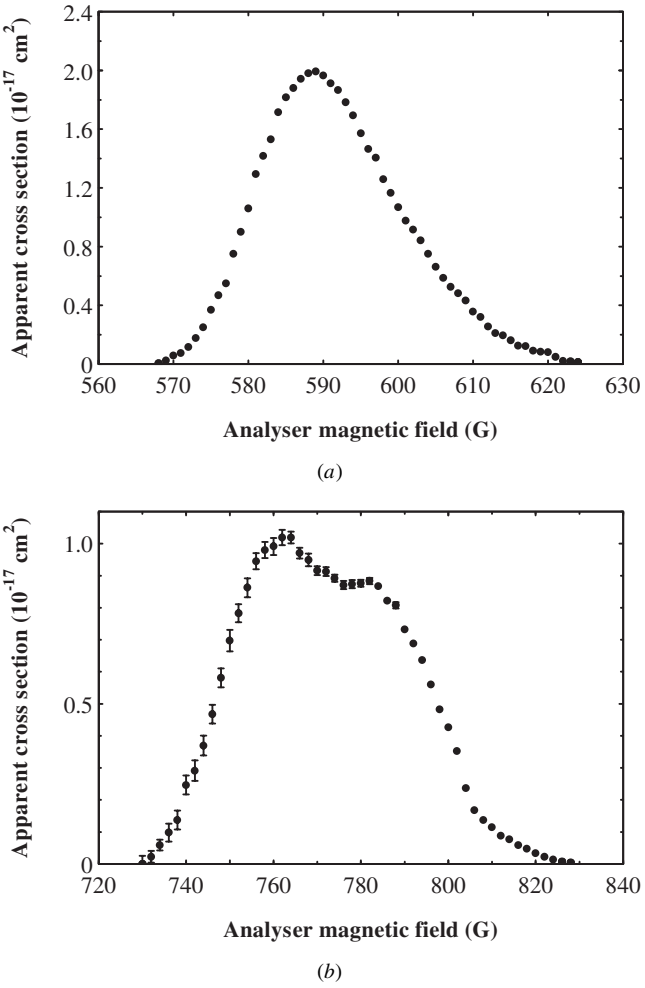

Figure 3. Apparent cross section for (*a*) C^+ and (*b*) O^+ production as a function of the analysing magnetic field observed at 120 eV electron energy.

to 620 G and presents no plateau and a single maximum near 590 G, corresponding to ions with zero KER. Apparent cross sections for C^+ production are measured at 590 G for electron energies from threshold to 2500 eV. Absolute cross sections are obtained after correction for the detection and transmission efficiencies. They are shown in figure 4.

In the low-electron energy region, ($E_e < 30$ eV), the shape of the curve is due to DE ($3a$) only. Around the maximum of the DE process, a wide plateau (extending from 30 to 100 eV) is most probably due to the opening of the DI channels ($2a$) or ($2f'$) around 40 eV.

Two thresholds corresponding to DE channels are observed at (9.5 ± 0.5) eV and at (15.0 ± 0.5) eV or, relative to the ground level of neutral CO_2, at (23.3 ± 0.5) and (28.8 ± 0.5) eV, respectively. The lower one is in good agreement with the results of Ehrhardt and Kresling (1967) (23.2 ± 0.2 eV), Crowe and McConkey (1974) (24.6 ± 1 eV) and Bussières and Marmet (1977) (22.7 ± 1 eV) obtained for C^+ production from electron impact CO_2 DI. The second threshold energy agrees with the values of (28.2 ± 0.2) and (27.8 ± 1) eV reported respectively by Ehrhardt and Kresling (1967) and Bussières and Marmet (1977). These authors also observed

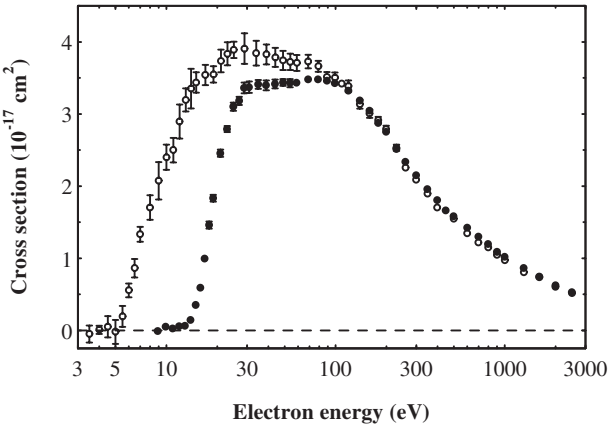

Figure 4. Absolute cross sections for C^+ (●) and O^+ (○) production.

that the cross section for the second channel is ten times larger than for the first one. This is confirmed in the present measurements by the presence of the very sharp change of slope corresponding to the second threshold. The maximum of the cross section (3.5×10^{-17} cm^2) is found at 80 eV. There are no other measurements or theoretical predictions to be compared with our data. However, it is interesting to note that the cross section for C^+ production from electron impact dissociation of neutral CO_2 is of the same order of magnitude. For instance, in recent measurements Tian *et al* (1998) obtained a maximum of 3.5×10^{-17} cm^2.

The low-lying electronic states of CO_2^+ are well established in terms of energy and stability (Hitchcock *et al* 1980, Eland 1972). The ground state ($X\ ^2\Pi_g$) and the two lowest excited electronic states ($A\ ^2\Pi_u$ and $B\ ^2\Sigma_u^+$) are stable against dissociation. These lie 3.8 and 4.3 eV above the ground ionic state, respectively. The $C\ ^2\Sigma_g^+$ which lies 5.6 eV above the ground state is fully predissociated and dissociates to give $CO^+ + O$ exclusively except for the lowest vibrational level which lies just below the $CO^+ + O$ formation energy. Higher-lying electronic states are less characterized. Photoionization experiments (Potts and Williams 1974) have shown the D and E states at energies of ∼8.9 and ∼13.5 eV, respectively. The D state lies below the dissociation limit to $C^+ + O_2$, and is expected to produce both $CO^+ + O$ and $O^+ + CO$ only. The E state lies above the dissociation limit for production of both $C^+ + O_2$ and $O_2^+ + C$. The lowest threshold energy observed in this experiment (9.5 ± 0.5) eV probably corresponds to the formation of the D state associated with vibrational excitation. The second dissociation threshold (15.0 ± 0.5) eV corresponds to dissociation of the E state.

The lower part of the electronic spectrum of CO_2^{2+} is governed by a high density of closely spaced electronic states (Hogreve 1995) and many of them should be present above the DI threshold. The present measurements show only the presence of this channel above 40 eV, but they do not allow any detailed discussion of this result.

Close to the dissociation threshold, the KER of product ions is nearly zero. The maximum available KER was measured at 120 eV, which is in a region where both DE and DI reactions are present. It was found to be relatively low (3 eV). Crowe and McConkey (1974), Velotta *et al* (1994) and Locht and Davister (1995) studied the fragment kinetic energy and angular distributions of C^+ from CO_2. They found essentially isotropic angular distributions. Velotta *et al* (1994) and Locht and Davister (1995) found a maximum of the energy distribution to be near zero energy, while Crowe and McConkey (1974) found a maximum of the distribution between 1 and 2 eV. This is also in agreement with the present KER observation.

4.3. O^+ production

O^+ ions are formed mainly in DE (3*b*) or in DI (2*b*). They may also result from post-collision dissociation of the diatomic ionic fragments O_2^+, CO^+ or even CO^{2+} and O_2^{2+} formed at higher electron energies. In addition, O_2^{2+} cannot be separated from O^+ by the magnet analyser. The magnetic field scan (figure 3(*b*)) shows that the O^+ spectrum is broader than the C^+ one, in particular at high electron energy. It is centred around 770 G (corresponding to ions with zero KER) and it extends from 730 to 830 G, at 120 eV incident electron energy. Furthermore, at high electron energy, it exhibits a weak local maximum near 785 G which could result from post-collision dissociation or from anisotropic angular distribution. This contribution does not exceed 15% of the overall signal.

Apparent cross sections for O^+ production are measured at 770 G. A non-vanishing signal is found below the expected threshold energy. The corresponding apparent cross section is estimated to be of the order of 1.0×10^{-18} cm^2 and extends down to the lower working limit of the electron gun. A similar behaviour was observed in earlier measurements. It was attributed to background modulation effects (Harrison 1966, Belic *et al* 1997). In that case, cross sections need to be corrected by subtracting this spurious contribution from the experimental results.

Absolute cross sections are also shown in figure 4. There are no other measurements or theoretical predictions to be compared with present data. The data again show a broad maximum, similar to the one observed for C^+ production: DE only plays a role in the low electron energy region and the plateau is most probably due to the opening of DI channels.

The maximum cross section is found to be 3.9×10^{-17} cm^2 around 30 eV. It is interesting to note that the cross section for O^+ produced by electron impact on neutral CO_2 lies in the same range (Crowe and McConkey 1974, Tian and Vidal 1998). The threshold energy is estimated to be (5.8 ± 0.5) eV, or 19.6 eV relative to the ground level of CO_2. This is in good agreement with the results of Eland and Danby (1968) (19.4 eV), Ehrhardt and Kresling (1967) (19.1 ± 0.4 eV) and Cuthbert *et al* (1968) (19.0 ± 0.4 eV) obtained for O^+ production from electron impact CO_2 DI.

The dissociation limit of CO_2^+ to form $O^+ + CO$ is at 19.38 eV relative to the CO_2 ground state (Price *et al* 1993). This means that 0.2 eV only is available for the dissociation close to the threshold. In this energy region it is most likely that predissociation via the C $^2\Sigma_g^+$ state occurs, in agreement with the conclusion of Eland (1972). Ehrhardt and Kresling (1967) have observed five DI thresholds leading to O^+ fragment from CO_2 at (19.1 ± 0.4), (22.4 ± 0.3), (24.3 ± 0.3) (28.3 ± 0.3) and (33.9 ± 0.3) eV. The KER was found to be 4.9 and 8.7 at 30 and 120 eV electron energy, respectively. By adding these KER values to the dissociation energy limit (19.38 eV), the energy of the corresponding dissociating CO_2^+ states are estimated to be 24.3 and 28.1 eV. These values almost coincide with the third and fourth thresholds reported by Ehrhardt and Kresling (1967). The dissociating states corresponding to these thresholds are still unknown. Other dissociation mechanisms could also contribute to the O^+ signal, but their identification was not possible in the present experiment.

5. Summary

Absolute cross sections for electron impact ionization of CO_2^+ and dissociation to C^+ and O^+ fragments have been measured in the energy range from threshold to 2.5 keV. For single ionization of CO_2^+ our data agree with previous measurements of Müller *et al* (1980). The threshold energy and KER determined for both the production of C^+ and O^+ are found to be in good agreement with the previously published data obtained in neutral CO_2 electron impact ionization experiments.

Acknowledgments

The authors are grateful to M Klosen, H Cherkani-Hassani, M Ould Abdellahi and C Alaime for their contributions to this work. EMB is grateful to Paul Maskens and his group for their financial support.

This paper is dedicated to the memory of M L'Host for his great contribution in the design and in the realization of the experimental set-up.

References

Andersen L H, Heber O, Kella D, Peterson H B, Vejby-Christensen L and Zaijfman D 1996 *Phys. Rev. Lett.* **77** 4891
Belic D S and Defrance P 1998 *XIX SPIG (Zlatibor, Yugoslavia)* (Contributed Papers) p 121
Belic D S, Yu D J, Siari A and Defrance P 1997 *J. Phys. B: At. Mol. Opt. Phys.* **30** 5535
Bussières N and Marmet P 1977 *Can. J. Phys.* **55** 1889
Crowe A and McConkey J W 1974 *J. Phys. B: At. Mol. Phys.* **7** 349
Cuthbert J, Farren J, Rao B S P and Preece E R 1968 *J. Phys. B: At. Mol. Phys.* **1** 62
Defrance P, Brouillard F, Claeys W and Wassenhove G 1981 *J. Phys. B: At. Mol. Phys.* **14** 103
Dibeler V H and Walker J A 1967 *J. Opt. Soc. Am.* **57** 1007
——1968 *Adv. Mass Spectrom* **4** 767
Djuric N, Chung Y S, Wallbank B and Dunn G H 1997 *Phys. Rev.* A **56** 2887
Dunn G H and Van Zyl B 1967 *Phys. Rev.* **154** 40
Eland J H D 1972 *Int. J. Mass Spectrom. Ion Phys*. **9** 397
Eland J H D and Danby C J 1968 *Int. J. Mass Spectrom. Ion Phys*. **1** 111
Ehrhardt H and Kresling A 1967 *Z. Naturf.* a **22** 2036
Field T A and Eland J H D 1993 *Chem. Phys. Lett.* **211** 436
Forck P, Grieser M, Habis D, Lampert A, Repnov R, Schwalm D, Wolf A and Zajfman D 1993 *Nucl. Instrum. Methods Phys. Res.* B **79** 273
Hall R I, McConkey A, Avaldi L, McDonald M A and King G C 1992 *J. Phys. B: At. Mol. Opt. Phys.* **25** 411
Harrison M F A 1966 *Br. J. Appl. Phys.* **17** 371
Hitchcock A P, Brion C E and Van der Weil M J 1980 *Chem. Phys.* **45** 461
Hogreve H 1995 *J. Phys. B: At. Mol. Opt. Phys.* **28** L263
Locht R and Davister M 1995 *Int. J. Mass Spectrom. Ion Process.* **144** 105
Märk T D and Hille E 1978 *J. Chem. Phys.* **69** 2492
McCulloh K E 1973 *J. Chem. Phys.* **59** 4250
Mitchell J B A and Hus H 1985 *J. Phys. B: At. Mol. Phys.* **18** 547
——1995 *Atomic and Molecular Processes in Fusion Edge Plasmas* ed R K Janev (New York: Plenum) p 259
Müller A, Salzborn E, Frodl R, Becker R and Klein H 1980 *J. Phys. B: At. Mol. Phys.* **13** L221
Newton A S and Sciamanna A F 1964 *J. Chem. Phys.* **40** 718
Peek J M 1967 *Phys. Rev.* **154** 52
Peterson J R *et al* 1998 *J. Chem. Phys.* **108** 1978
Potts A W and Williams T A 1974 *J. Electron Spectrosc. Relat. Phenom.* **3** 3
Price S D, Rogers S A and Leone S R 1993 *J. Chem. Phys.* **98** 9455
Schulz P A, Gregory D C, Meyer F W and Phaneuf R A 1986 *J. Chem. Phys.* **85** 3386
Siari A, Belic D S, Defrance P and Rachafi S 1999 *J. Phys. B: At. Mol. Opt. Phys.* **32** 587
Tian C and Vidal C R 1998 *J. Chem. Phys.* **108** 927
Tsai B P and Eland J H D 1980 *Int. J. Mass Spectrom. Ion Phys.* **36** 143
Van der Donk P, Yousif F B and Mitchell J B A 1991 *Phys. Rev.* A **43** 5971
Van Zyl B and Dunn G H 1967 *Phys. Rev.* **163** 43
Velotta R, Girolamo P, Di Beradi V, Spinelli N and Armenante M 1994 *J. Phys. B: At. Mol. Opt. Phys.* **27** 2051
Zambra M, Belic D S, Defrance P and Yu D J 1994 *J. Phys. B: At. Mol. Opt. Phys.* **27** 2383